ACADEMIA ROMÂNĂ
Revue Roumaine de Chimie
http://web.icf.ro/rrch/

Rev. Roum. Chim.,
2019, *64*(9), 817-828
DOI: 10.33224/rrch.2019.64.9.09

SYNTHESIS OF IRON(III) OXIDE NANOPARTICLES *VIA* SIMPLE AND CHEAP PROCEDURES FOR ADSORPTION OF ENVIRONMENTALLY HARMFUL TOXIC HEAVY METALS

Ahmed ALHADHRAMI,[a] Abdel Majid A. ADAM,[a]
Abdulraheem S. A. ALMALKI,[a] and Moamen S. REFAT[a,b,*]

[a]Department of Chemistry, Faculty of Science, Taif University, Al-Hawiah, Taif, P.O. Box 888 Zip Code 21974, Saudi Arabia
[b]Department of Chemistry, Faculty of Science, Port Said University, Port Said, Egypt

Received March 23, 2019

In aqueous media at ~50 °C, two new iron(III) complexes, $[Fe_3(\mu\text{-}CO_3)(NH_3)(\mu\text{-}OH)_2(H_2O)_5(\mu\text{-}H_2O)(OH)_4]Cl{\cdot}6H_2O$ and $[Fe_3(\mu\text{-}CO_3)(NH_3)(\mu\text{-}OH)_2(H_2O)_5(\mu\text{-}H_2O)(OH)_4]NO_3{\cdot}6H_2O$, were synthesized from $FeCl_3{\cdot}6H_2O$ and $Fe(NO_3)_3{\cdot}9H_2O$ with urea, a simple organic compound. These complexes were used as the primary precursors for iron(III) oxide (Fe_2O_3) nanoparticle (NP) preparation via a thermal decomposition route at a low temperature (600 °C) in a static air atmosphere. The complexes of iron(III) were analyzed through FTIR spectroscopy, thermal properties, conductivity and magnetic moment measurements, while the oxide materials were characterized through UV-Vis, XRD and SEM measurements. The study also aimed to investigate the performance and capacity of Fe_2O_3 NPs for the removal of some heavy metals, such as cadmium (Cd^{2+}), lead (Pb^{2+}), and mercury (Hg^{2+}) ions. The optimum adsorbent dose, contact time, and pH values for maximum Cd^{2+}, Pb^{2+} and Hg^{2+} metal ion removal were identified. The adsorption behavior was found to be highly pH-dependent, and the Fe_2O_3 NPs selectively absorbed Cd^{2+}, Pb^{2+} and Hg^{2+} metal ions from wastewater.

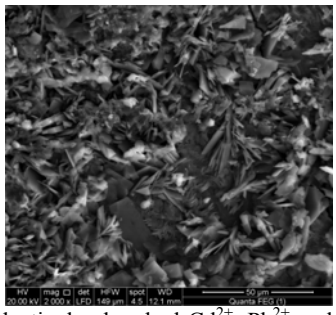

INTRODUCTION

Industrial development has led to an increase in pollution, including increased heavy metal release into the environment, which represents a serious global environmental problem.[1] Activated carbon is often used as an adsorbent in order to remove heavy metals from waste streams. Despite the widespread use of activated carbon to treat sewage and water, activated carbon remains an expensive option.[2,3] Recently, commercially available, low-cost alternatives to activated carbon have become available, and their use and ability to remove heavy metals must be evaluated. Metal oxides have important applications in several fields, such as materials science, physics, and chemistry,[4–10] and these oxides are used to manufacture precision circuits, catalysts, anti-corrosion coatings, sensors, and fuel cells. In order to control environmental pollution, substances containing oxides are used to remove carbon dioxide and the nitrogen and sulfur oxides that are emitted during the combustion of fossil fuels.[11] Furthermore, metal oxides are used to manufacture the different types of semiconductors that are used in computer chips.[12] Currently, inorganic scientists are exploring new uses and applications for metal oxide materials.[13–15] Iron (III) oxide (Fe_2O_3) nanoparticles (NPs) have large surface areas and can be easily linked with various chemicals.[16–18]These properties facilitate their use in several promising applications, such as environmental treatments and the development of magnetic recording devices, sensors, electronic devices, and catalysts.

* Corresponding author: msrefat@yahoo.com

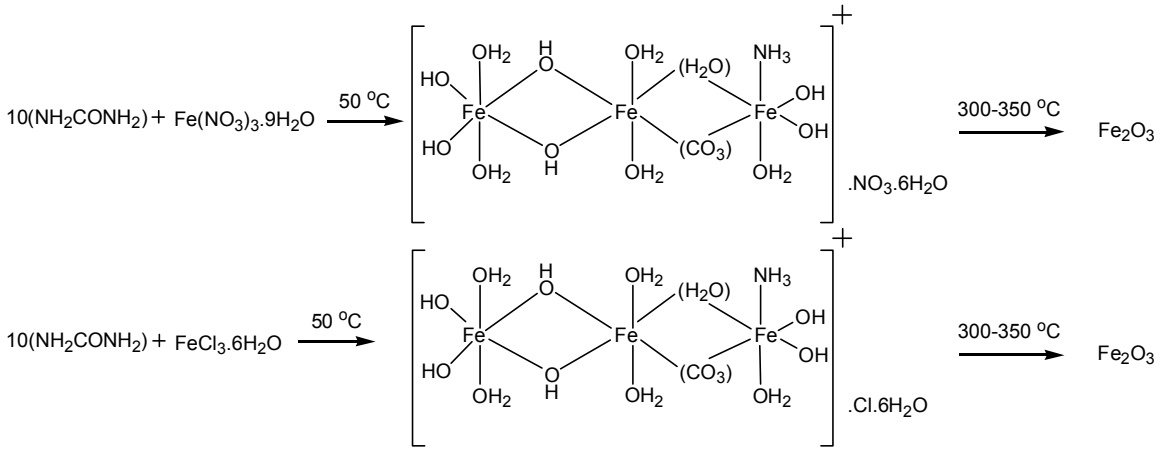

Scheme 1 – Preparations of the iron(III) complexes and Fe_2O_3 product.

Several studies have reported Fe_2O_3 synthesis and characterization in the presence of urea. For examples, Ocana *et al.*[19] described a method for Fe_2O_3 particle preparation by precipitation from aqueous solutions of $FeCl_3$, $Fe(ClO_4)_3$, and $Fe(NO_3)_3$ at 100 °C in the presence of urea. Bakardjieva *et al.*[20] prepared uniform spherical hydrous Fe_2O_3 particles through urea decomposition of the homogeneous precipitation of $Fe_2(SO_4)_3$. Asuha *et al.*[21,22] developed a new method for the preparation of Fe_2O_3 nanopowder via thermal decomposition of the $[FeCON_2H_4)_6](NO_3)_3$ complex, and they studied the effects of synthetic routes of this complex on the resulting Fe_2O_3 nanopower.[23] Jović *et al.*[24] prepared Fe_2O_3 NPs via hydrolysis of $Fe(NO_3)_3$ in the presence of urea and oleic acid. Liang *et al.*[25] described an easy, simple, and economical method for preparation of Fe_2O_3 microflowers via an urea-assisted hydrothermal synthetic route. They used the Fe_2O_3 product as an adsorbent for water treatment with a potential adsorbent capacity for As (V) and Cr (VI) heavy metal ion removal. Fe_2O_3 is reported to remove lead (Pb),[26] arsenic (As),[27] and mercury (Hg)[28] from water. Wang *et al.*[29] used $FeCl_3$ to prepare Fe_2O_3 and Fe_3O_4 nanostructures with different morphologies via an ethylene glycol (EG)-mediated process with the assistance of urea and cetyl trimethyl ammonium bromide (CTAB). They used these oxides to adsorb Cr(VI) ions with a maximum adsorption capacity equal to 6.9 mgg^{-1}. This value was higher than that of commercial bulk Fe_2O_3. In this study, we aimed to prepare two new proposed iron (III) complexes from the reaction of $FeCl_3{\cdot}6H_2O$ and $Fe(NO_3)_3{\cdot}9H_2O$ salts with urea at ~50 °C. These proposed complexes were $[Fe_3(\mu\text{-}CO_3)(NH_3)(\mu\text{-}OH)_2(H_2O)_5(\mu\text{-}H_2O)(OH)_4]Cl{\cdot}6H_2O$ and $[Fe_3(\mu\text{-}CO_3)(NH_3)(\mu\text{-}OH)_2(H_2O)_5(\mu\text{-}H_2O)(OH)_4]NO_3{\cdot}\ 6H_2O$, which were thermally decomposed at 600 °C in air atmosphere to produce Fe_2O_3 NPs. The capability of the resulting Fe_2O_3 to purify water contaminated with heavy elements resulting from industrial waste, such as Cd, Pb, and Hg was investigated.

EXPERIMENTAL

1. General

Urea and metal salts, $FeCl_3{\cdot}6H_2O$, $Fe(NO_3)_3{\cdot}9H_2O$, $Cd(NO_3)_2$, $Pb(CH_3COO)_2$, and $Hg(NO_3)_2$, were received from Sigma-Aldrich and used as obtained. The solvents were spectroscopic grade. Elemental analyses of %N, %H, and %C were performed using a Perkin Elmer CHN 2400 instrument. The iron metal content was obtained using an atomic absorption spectrometer model PYE-UNICAM SP 1900. The molar conductivity of the iron(III) complexes with a 10^{-3} mol/cm^3 concentration were obtained with a Jenway 4010 conductivity meter. A UV2–Unicam UV/Vis spectrophotometer was used to record the electronic absorption of the Fe_2O_3 NPs (200-800 nm). A Sherwood Scientific model instrument was used to measure the magnetic susceptibilities of the samples at room temperature via the Gouy method [30]. The IR spectra (KBr discs) were obtained on a Bruker FT-IR spectrophotometer within the range 400-4000 cm^{-1}. Thermogravimetric (TG) curves were obtained using a Shimadzu computerized thermal analysis system (TGA-50H). The XRD patterns were collected on an X Pert Philips X-ray diffractometer. The SEM micrographs were visualized using a Jeol Jem–1200 EX II Electron microscope (25 kV).

2. Synthesis

The two new proposed iron (III) complexes, $[Fe_3(\mu\text{-}CO_3)(NH_3)(\mu\text{-}OH)_2(H_2O)_5(\mu\text{-}H_2O)(OH)_4]Cl{\cdot}6H_2O$ and $[Fe_3(\mu\text{-}CO_3)(NH_3)(\mu\text{-}OH)_2(H_2O)_5(\mu\text{-}H_2O)(OH)_4]NO_3{\cdot}6H_2O$ were prepared by mixing equal volumes (100 mL) of $FeCl_3{\cdot}6H_2O$ or $Fe(NO_3)_3{\cdot}9H_2O$ (0.01 mol) with urea (0.1 mol) at 50 °C, respectively. These complexes began to settle as a brown precipitate after a long heating time of approximately 16 hours. After separation by filtration, the precipitates were washed several times with hot water to remove all urea residue and then dried in a vacuum dissector over P_2O_5 for approximately four days.

$[Fe_3(\mu\text{-}CO_3)(NH_3)(\mu\text{-}OH)_2(H_2O)_5(\mu\text{-}H_2O)(OH)_4]Cl{\cdot}6H_2O$; complex 1: yield 73%. M.p. > 250 °C. Anal.: (Calc.) Found, %: C, (2.01) 1.99; H; (5.52) 5.50; N, (2.34) 2.30; Fe, (28.02) 27.98. $\Lambda_M = 71\ \Omega^{-1}{\cdot}cm^2{\cdot}mol^{-1}$.

$[Fe_3(\mu\text{-}CO_3)(NH_3)(\mu\text{-}OH)_2(H_2O)_5(\mu\text{-}H_2O)(OH)_4]NO_3{\cdot}6H_2O$; complex 2: yield 76%. M.p. > 250 °C. Anal.: (Calc.) Found, %: C, (1.92) 1.89; H; (5.28) 5.25; N, (4.48) 4.42; Fe, (26.83) 26.76. $\Lambda_M = 64\ \Omega^{-1}{\cdot}cm^2{\cdot}mol^{-1}$.

The Fe_2O_3 NPs were prepared by the thermal decomposition of the iron(III) complexes at 600 °C in an air oxygen atmosphere.

3. Adsorption experiments

The adsorption experiments were performed in 50 mL glass bottles using 50 mg of the Fe_2O_3 product as the adsorbent in 30 mL of stock aqueous solutions of Cd^{2+}, Pb^{2+} and Hg^{2+} ions. The stock solutions of Cd^{2+}, Pb^{2+} and Hg^{2+} were prepared by dissolving a suitable amount (20 mg) of $Cd(NO_3)_2$, $Pb(CH_3COO)_2$ or $Hg(NO_3)_2$ in 100 mL deionized water. The contents in each glass bottle were shaken for different times (10, 20, 30, 40, 50 or 60 minutes). After each mixing time, the Fe_2O_3 were anchored on the bottom of the bottle, and the residue was removed by filtration. Atomic absorption spectroscopy was used to determine the concentration of the unabsorbed heavy metal ions in the supernatant liquid. The pH of the solutions was adjusted using sodium hydroxide (0.01 N) or hydrochloric acid (0.01 N).

RESULTS AND DISCUSSION

1. Preface

The two new brown solid complexes, $[Fe_3(\mu\text{-}CO_3)(NH_3)(\mu\text{-}OH)_2(H_2O)_5(\mu\text{-}H_2O)(OH)_4]Cl{\cdot}6H_2O$ and $[Fe_3(\mu\text{-}CO_3)(NH_3)(\mu\text{-}OH)_2(H_2O)_5(\mu\text{-}H_2O)(OH)_4]NO_3{\cdot}6H_2O$ were obtained in aqueous solutions at a moderate temperature (~ 50 °C) via the reaction of urea with $FeCl_3{\cdot}6H_2O$ and $Fe(NO_3)_3{\cdot}9H_2O$, respectively. These solid complexes were identified through their elemental analyses and infrared spectra. The thermal analyses (TG and DTG) of the two complexes were also used to establish their proposed structures. The Fe_2O_3 NPs were prepared by thermal decomposition of the iron(III) complexes at 600 °C in an oxygen atmosphere. The proposed structures of the iron(III) complexes before and after the thermal decomposition were investigated using spectroscopic and physical measurements. Scheme 1 shows the proposed route for the preparation of the iron (III) complexes and Fe_2O_3 product.

2. FTIR study

Table 1 gives the IR vibrational assignments of the $[Fe_3(\mu\text{-}CO_3)(NH_3)(\mu\text{-}OH)_2(H_2O)_5(\mu\text{-}H_2O)(OH)_4]Cl{\cdot}6H_2O$ and $[Fe_3(\mu\text{-}CO_3)(NH_3)(\mu\text{-}OH)_2(H_2O)_5(\mu\text{-}H_2O)(OH)_4]NO_3{\cdot}6H_2O$ complexes. The infrared spectra of the two iron(III) complexes have common features: *(i)* the bands due to the coordinated urea were absent; *(ii)* a number of bands observed at approximately 1387 and 1499 cm^{-1} were related to the bond vibrations of ν(C-O) in the CO_3 group, and these bands were characteristic of the bridged carbonato ligand [31]; *(iii)* a set of bands attributed to the stretching vibrations of uncoordinated H_2O molecules and bridged hydroxide ligands were observed in the region of 3452–3354 cm^{-1};[31,32] *(iv)* the band observed at 3195–3202 cm^{-1} was associated with the stretching motion of the ammine group; NH_3.[32]

The IR spectrum of the $[Fe_3(\mu\text{-}CO_3)(NH_3)(\mu\text{-}OH)_2(H_2O)_5(\mu\text{-}H_2O)(OH)_4]\ NO_3{\cdot}6H_2O$ complex shows a set of bands at 1387 and 829 cm^{-1} with strong-to-medium intensities, and they were characteristic of the ionic nitrate group; NO_3^-.[31,33] The IR spectra of both iron(III) complexes suggest the existence of the same cationic ion complex; $[Fe_3(\mu\text{-}CO_3)(NH_3)(\mu\text{-}OH)_2(H_2O)_5(\mu\text{-}H_2O)(OH)_4]^+$, but the anionic counter ion differs, *e.g.*, NO_3^- or Cl^-, which agrees with the elemental analysis data. Heating of an aqueous mixture of $FeCl_3{\cdot}6H_2O$ or $Fe(NO_3)_3{\cdot}9H_2O$ with urea formed the $[Fe_3(\mu\text{-}CO_3)(NH_3)(\mu\text{-}OH)_2(H_2O)_5(\mu\text{-}H_2O)(OH)_4]^+$ ion as follows: Fe^{3+} ions complexed with urea to form the parent complex [34] of the type $[Fe(urea)_6]X_3$ (where X = Cl^- or NO_3^-) at room temperature, but at moderate temperatures, the following reactions may occur:

$$3[Fe(NH_2CONH_2)_6]Cl_3 + 37H_2O \rightarrow [Fe_3(\mu\text{-}CO_3)(NH_3)(\mu\text{-}OH)_2(H_2O)_5(\mu\text{-}H_2O)(OH)_4]\ Cl{\cdot}6H_2O + 8HCl + 35NH_3 + 17CO_2$$

$$3[Fe(NH_2CONH_2)_6](NO_3)_3 + 37H_2O \rightarrow [Fe_3(\mu\text{-}CO_3)(NH_3)(\mu\text{-}OH)_2(H_2O)_5(\mu\text{-}H_2O)(OH)_4]\ NO_3{\cdot}6H_2O + 8HNO_3 + 35NH_3 + 17CO_2$$

The bands associated with the bridged carbonato ligand in the two iron(III) complexes are assigned as follows. The symmetric $\nu_s(CO_2)$, ν_1, is observed at 1499 cm^{-1} for the two complexes, while the anti-symmetric $\nu_{as}(CO_2)$, ν_4, is observed at 1387 cm^{-1} for the two complexes. The ν(C-O), ν_2, vibration in the two complexes appears as one medium intensity band at 1031 cm^{-1}. The $\delta(CO_2)$ vibration in the two complexes appears as medium-weak intensity bands at 829 and 768 cm^{-1}. The assignments of these bands agree well with those known for the related bridged carbonate complexes.[31] The various ν(O-H) vibrations of the uncoordinated water molecules and the bridged hydroxide ligand in the two complexes are clearly observed as a number of weak broad bands in the 3452–3354 cm^{-1} region, while the associated bending motions of the coordinated water molecules are located as expected at 1642 and 1635 cm^{-1}. The bending vibration of the ammine group, $\delta(NH_3)$, was assigned to the bands at 1567 and ~ 1160 cm^{-1}, while that of the $\nu(NH_3)$ vibration was observed as a weak broad band in its characteristic place at ~ 3200 cm^{-1}.

3. Thermal analysis study

The TG and DTG analyses were performed for the $[Fe_3(\mu\text{-}CO_3)(NH_3)(\mu\text{-}OH)_2(H_2O)_5(\mu\text{-}H_2O)(OH)_4]Cl{\cdot}6H_2O$ and $[Fe_3(\mu\text{-}CO_3)(NH_3)(\mu\text{-}OH)_2(H_2O)_5(\mu\text{-}H_2O)(OH)_4]NO_3{\cdot}6H_2O$ complexes under an air atmosphere (Fig. 1). The $[Fe_3(\mu\text{-}CO_3)(NH_3)(\mu\text{-}OH)_2(H_2O)_5(\mu\text{-}H_2O)(OH)_4]Cl{\cdot}6H_2O$ complex thermally degraded in four steps. The first step occurs at 48 °C, which represents the dehydration of four uncoordinated water molecules. The actual weight loss from this degradation step was 12.0%, while the theoretical weight loss is 12.04%. The second step of the decomposition occurs at a maximum temperature of 221 °C. The IR spectrum (Fig. 2a,b) of the thermal product at this temperature clearly indicates the formation of the NCO^- group with its characteristic ν(N≡C) at ~ 2200 cm^{-1},[35] due to the combination of NH_3 and CO_3 at high temperatures.[36] This important result strongly supports our conclusion concerning the proposed structures of these complexes under investigation. Nine uncoordinated water molecules were lost in the second step (found, 27.0%; calc., 27.09%). The third step occurs at a maximum temperature of 412 °C. The weight loss in the third step is 15.0% due to the loss of $3H_2O$ and HCl, which is in agreement with the theoretical weight loss value of 15.13%.

The last decomposition step occurs at 540 °C and is accompanied by a weight loss of 6.5%, corresponding to the loss of $½O_2$ and CN molecules as a result of the degradation of the NCO group, to give Fe_2O_3. The loss of H_2O molecules in the degradation steps indicates that H_2O molecules with different lattice proposed structures exist in the complex. According to the above discussion, the decomposition mechanism of the $[Fe_3(\mu\text{-}CO_3)(NH_3)(\mu\text{-}OH)_2(H_2O)_5(\mu\text{-}H_2O)(OH)_4]Cl{\cdot}6H_2O$ complex is as follows:

$$[Fe_3(\mu\text{-}CO_3)(NH_3)(\mu\text{-}OH)_2(H_2O)_5(\mu\text{-}H_2O)(OH)_4]Cl{\cdot}6H_2O \xrightarrow{48^oC} [Fe_3(\mu\text{-}CO_3)(NH_3)(\mu\text{-}OH)_2(H_2O)_5(\mu\text{-}H_2O)(OH)_4]Cl{\cdot}2H_2O + 4H_2O$$

$$[Fe_3(\mu\text{-}CO_3)(NH_3)(\mu\text{-}OH)_2(H_2O)_5(\mu\text{-}H_2O)(OH)_4]Cl{\cdot}2H_2O \xrightarrow{221^oC} [Fe_3(NCO)(OH)_7]{\cdot}Cl + 9H_2O$$

$$[Fe_3(NCO)(OH)_7]{\cdot}Cl + 9H_2O \xrightarrow{412^oC} [Fe_3(NCO)(O)_4] + 3H_2O + HCl$$

$$[Fe_3(NCO)(O)_4] \xrightarrow{421^oC} (Fe_2O_3)_{1.5} + ½O + CN$$

The IR spectrum of the final thermal degradation product for this complex supports the suggested mechanism. The IR spectrum shows the absence of the bands of uncoordinated water molecules and carbonate, ammine and hydroxyl groups and the presence of two strong bands of Fe_2O_3,[31] at 565 and 466 cm^{-1}, which are related to Fe-O bond vibrations.

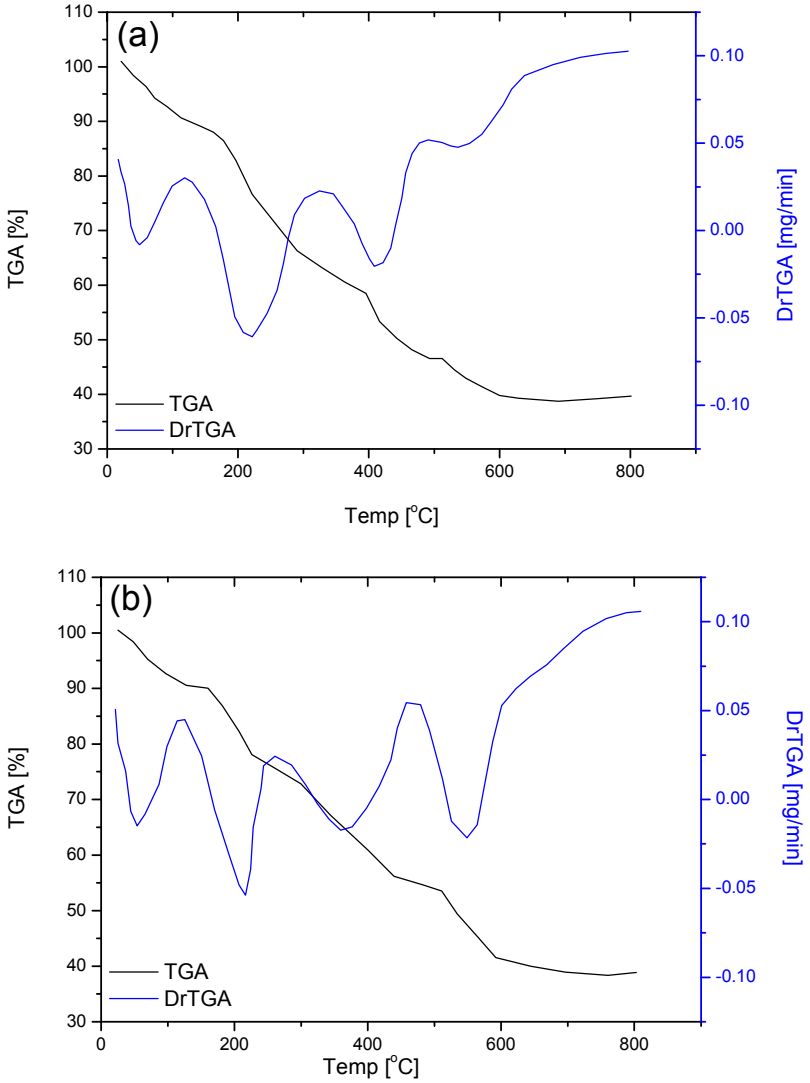

Fig. 1 – TGA/DTG curves of iron(III) complexes, (a): $[Fe_3(\mu\text{-}CO_3)(NH_3)(\mu\text{-}OH)_2(H_2O)_5(\mu\text{-}H_2O)(OH)_4]Cl{\cdot}6H_2O$ and (b): $[Fe_3(\mu\text{-}CO_3)(NH_3)(\mu\text{-}OH)_2(H_2O)_5(\mu\text{-}H_2O)\ (OH)_4]NO_3{\cdot}6H_2O$.

Table 1

IR frequencies (cm^{-1}) and band assignments for $[Fe_3(\mu\text{-}CO_3)(NH_3)(\mu\text{-}OH)_2(H_2O)_5(\mu\text{-}H_2O)(OH)_4]Cl{\cdot}6H_2O$ (Complex 1), and $[Fe_3(\mu\text{-}CO_3)(NH_3)(\mu\text{-}OH)_2(H_2O)_5\ (\mu\text{-}H_2O)(OH)_4]NO_3{\cdot}6H_2O$ (Complex 2)

Frequency (cm^{-1})		**Assignments**
Complex 1	**Complex 2**	
3452	3452	ν(O- H); (Fe-OH)
3355	3354	ν (O - H); H_2O
3195	3202	ν (N-H); NH_3
1635	1642	δ (H_2O)
1567	1567	δ (NH_2); NH_3
1499	1499, 1387	ν (C-O); CO_3^{2-} ν (N-O); NO^{3-}
1167	1152	δ (NH_2); NH_3
1031	1031	ν(C-O); CO_3^{2-}
768	829	δ (CO_2); CO_3^{2-}
632	768, 631	δ (NO_2); NO_3^- δ (CO_2); CO_3^{2-}
549	549	ν (Fe-O)
466	466	ν (Fe-N)

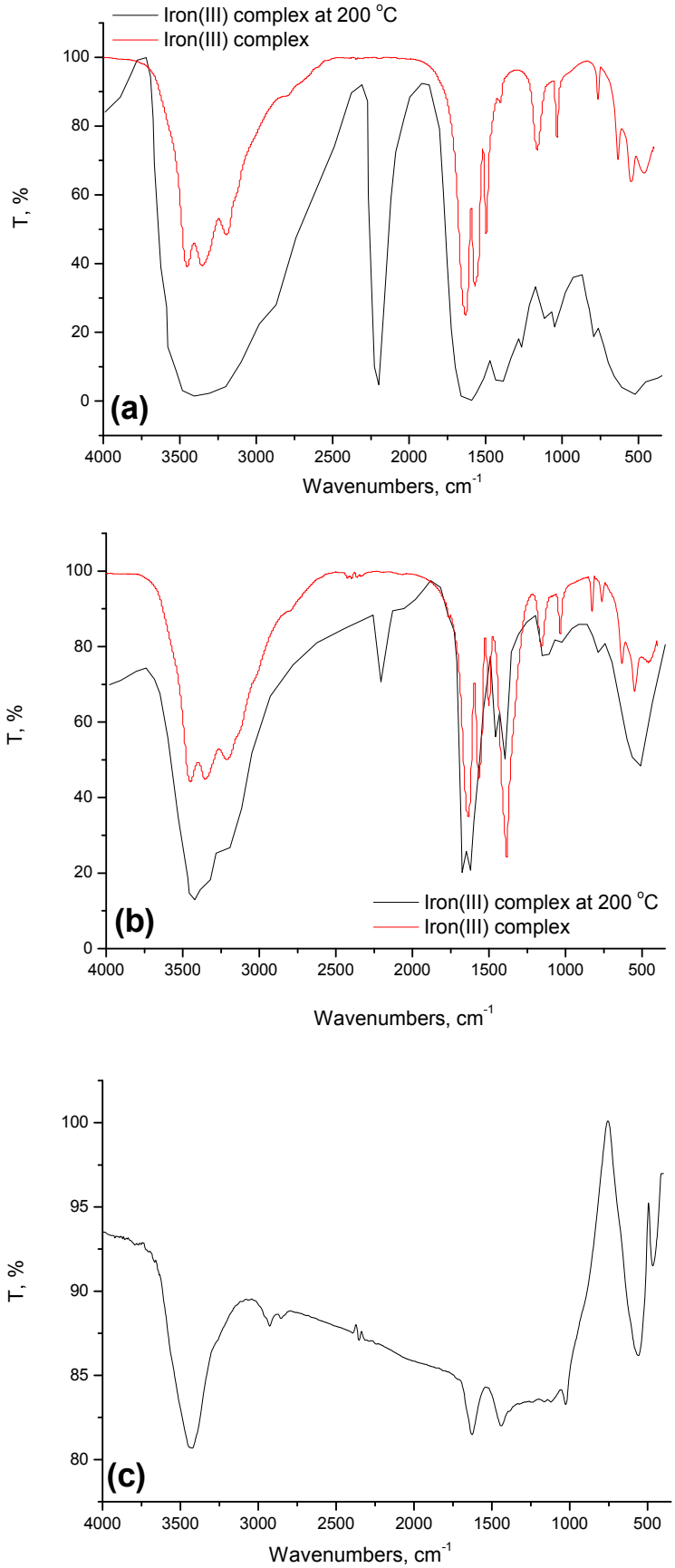

Fig. 2 – IR spectrum of (a) iron(III) complex 1 in normal and at 200°C, (b) iron(III) complex 2 in normal and at 200°C and (c) iron(III) complexes at 600°C.

The thermal decomposition of the $[Fe_3(\mu\text{-}CO_3)(NH_3)(\mu\text{-}OH)_2(H_2O)_5(\mu\text{-}H_2O)(OH)_4]NO_3{\cdot}6H_2O$ complex proceeds via four decomposition stages. The first two stages of degradation occur at the maximum temperatures of 52 and 214 °C and were accompanied by the formation of the NCO^- group, which is similar to the related complex $[Fe_3(\mu\text{-}CO_3)(NH_3)(\mu\text{-}OH)_2(H_2O)_5(\mu\text{-}H_2O)(OH)_4]Cl{\cdot}6H_2O$, and a weight loss of 28.0% (calc., 27.38%) corresponds to the loss of the six uncoordinated H_2O molecules and HNO_3 in the gaseous form. The third step occurs at a maximum temperature of 358 °C with a weight loss of 17.0% (calc., 27.29%) and was associated with the loss of six H_2O molecules. The fourth step occurs at a maximum temperature of 549 °C with a weight loss of 17.00%, which is close to the theoretical weight loss value of 16.97%, and was accompanied by the loss of HCNO and 3½ H_2O molecules. The loss of water molecules at relatively high temperatures may be related to the expected strong H-bonding involving both the OH^- and water molecules. According to the above discussion, the decomposition mechanism of the $[Fe_3(\mu\text{-}CO_3)(NH_3)(\mu\text{-}OH)_2(H_2O)_5(\mu\text{-}H_2O)(OH)_4]NO_3{\cdot}6H_2O$ complex is as follows:

$$[Fe_3(\mu\text{-}CO_3)(NH_3)(\mu\text{-}OH)_2(H_2O)_5(\mu\text{-}H_2O)(OH)_4]NO_3{\cdot}6H_2O \xrightarrow{52,214^oC} [Fe_3(NCO)(H_2O)_6(OH)_8] + 6H_2O + HNO_3$$

$$[Fe_3(NCO)(H_2O)_6(OH)_8] \xrightarrow{358^oC} [Fe_3(NCO)(OH)_8] + 6H_2O$$

$$[Fe_3(NCO)(OH)_8] \xrightarrow{549^oC} (Fe_2O_3)_{1.5} + 3½H_2O + HNCO$$

4. Molar conductance and magnetic moments

The molar conductance's for the $[Fe_3(\mu\text{-}CO_3)(NH_3)(\mu\text{-}OH)_2(H_2O)_5(\mu\text{-}H_2O)(OH)_4]Cl{\cdot}6H_2O$ and $[Fe_3(\mu\text{-}CO_3)(NH_3)(\mu\text{-}OH)_2(H_2O)_5(\mu\text{-}H_2O)(OH)_4]NO_3{\cdot}6H_2O$ complexes were 71 and 64 $\Omega^{-1}cm^2\ mol^{-1}$ in DMSO solvent, respectively, indicating their electrolytic nature.[37] The conductance values revealed the presence of one Cl^- or NO_3^- anion outside the coordination sphere. The effective magnetic moment μ_{eff} of the these complexes was between 5.73-5.81 BM, which indicates a high-spin octahedral geometry.[38]

5. XRD, EDX and SEM studies

Figure 3 shows the X-ray powder diffraction patterns of the Fe_2O_3 product obtained from the thermal decomposition of the $[Fe_3(\mu\text{-}CO_3)(NH_3)(\mu\text{-}OH)_2(H_2O)_5(\mu\text{-}H_2O)(OH)_4]NO_3{\cdot}6H_2O$ complex at 600 °C. The diffraction patterns are well indexed and assigned to the hexagonal phase $\alpha\text{-}Fe_2O_3$. The 2θ peaks at 24.08, 33.09, 35.61, 40.83, 49.40, 54.06, 57.60, 62.25 and 63.93 can be attributed to the (012), (104), (110), (113), (024), (116), (018), (214) and (300) crystal planes, respectively (Powder Diffraction Standards-JCPDS card No. 80-2377).[39] The energy dispersive X-ray (EDX) spectrum shows that only Fe and O elements are present in the measured $\alpha\text{-}Fe_2O_3$ product. This observation is supported by the absence of any XRD pattern other than nanocrystalline $\alpha\text{-}Fe_2O_3$. The average particle size of the $\alpha\text{-}Fe_2O_3$ NPs was calculated at the highest maximum peak (104) using the Scherrer equation (1)[40] and was found to be ~ 14 nm.

$$D = (K\lambda)/(\beta\cos\theta) \quad (1)$$

where θ is the Bragg diffraction angle, K is a constant (0.94 for Cu grid), β is the integral peak width, λ is the X-ray wavelength (1.5406 Å), and D is the particle size. The scanning electron microscopy (SEM) micrograph of the $\alpha\text{-}Fe_2O_3$ NPs is shown in Figure 4. The SEM micrograph of the $\alpha\text{-}Fe_2O_3$ NPs shows a medium degree of agglomeration and particles with a uniform size distribution in the form of flat sheets.

6. Electronic and optical band gap energy studies

The electronic spectrum of the $\alpha\text{-}Fe_2O_3$ NPs was scanned using a UV-Vis spectrometer and shown in Figure 5. This spectrum shows broad absorption peaks at 299 and 362 nm, which can be attributed to the absorption and scattering of light by the $\alpha\text{-}Fe_2O_3$ NPs.[41]. The optical band gap energy (E_g) of the $\alpha\text{-}Fe_2O_3$ NPs was estimated from the electronic spectrum using the Tauc relation (equation 2).[42]

$$\alpha h\nu = A(h\nu - E_g)^n \quad (2)$$

where A is a constant, hν is the photon energy, E_g is the energy gap, and n = ½ for an allowed direct transition. The band gap energy was determined from the plot of the relationship between $(\alpha h\nu)^{½}$ and hν, and the value was (E_g = 2.53 eV). This

value is higher than that of bulk Fe_2O_3 (E_g = 2.14-2.20 eV).[43] Therefore, the increase in the energy band gap compared with that of the bulk material is due to the presence of Fe_2O_3 in nano-range.[44]

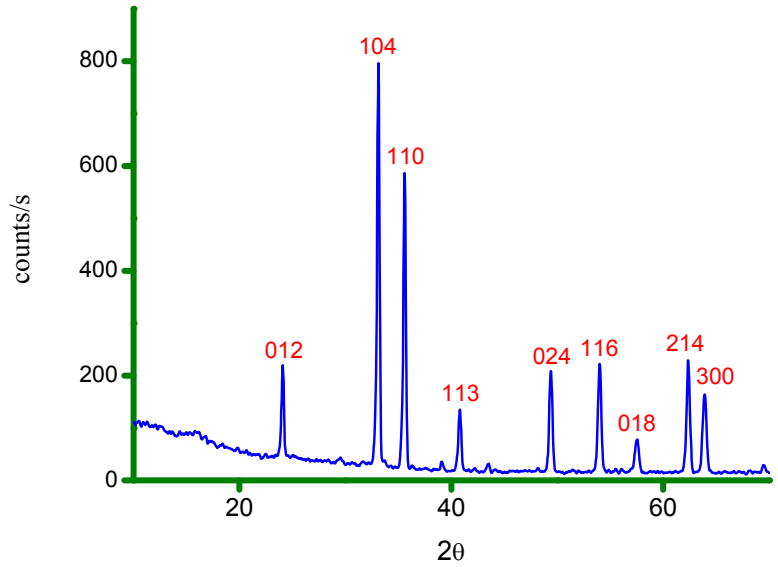

Fig. 3 – XRD patterns of the synthesized α-Fe_2O_3 NPs.

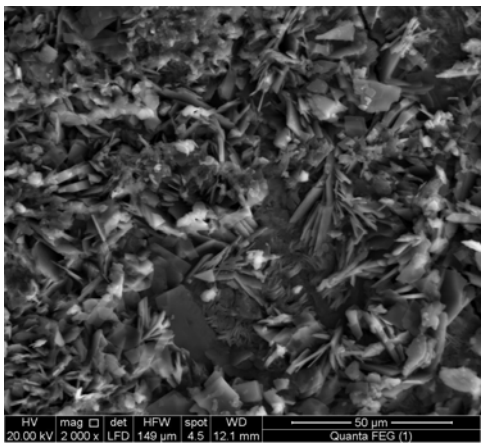

Fig. 4 – SEM micrographs of the synthesized α-Fe_2O_3 NPs.

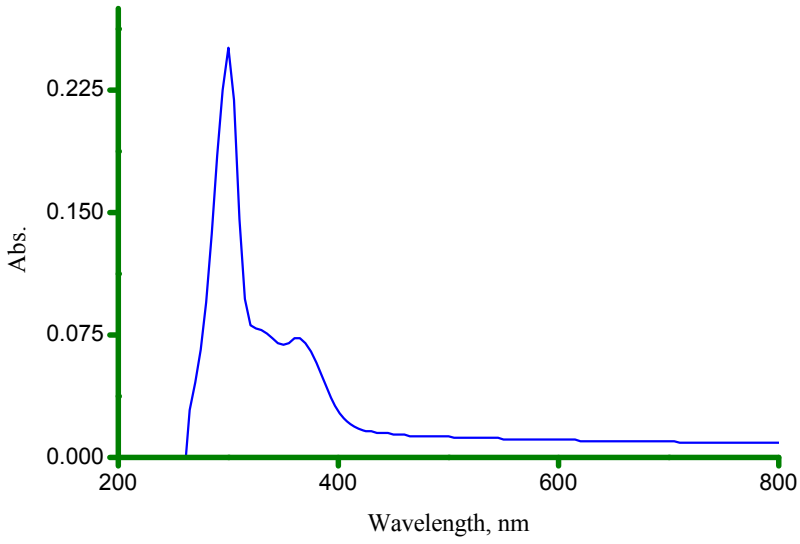

Fig. 5 – UV-Visible spectrum of the synthesized α-Fe_2O_3 NPs.

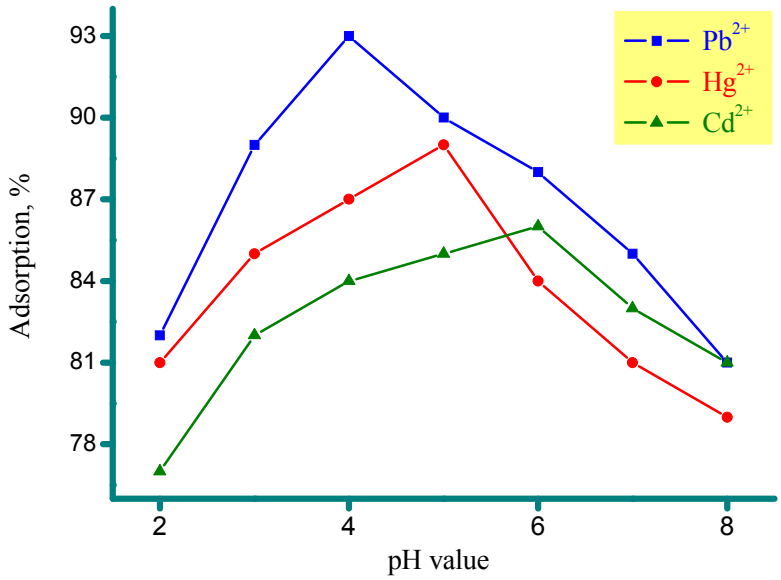

Fig. 6 – Effect of pH values on the adsorption of Pb^{2+}, Hg^{2+} and Cd^{2+} ions by α-Fe_2O_3 NPs.

7. Factors affecting the removal efficiency of heavy metals

1. Effect of the pH

The influence of the pH is an important factor in the removal of heavy metal ions using Fe_2O_3 NPs. The effect of the pH on the removal of Pb^{2+}, Hg^{2+} and Cd^{2+} ions by α-Fe_2O_3 NPs was examined within the pH range of 2.00–8.00, and illustrated in Figure 6. It has been found that approximately 93, 89 and 86% of the Pb^{2+}, Hg^{2+} and Cd^{2+} ions, respectively, were adsorbed on the α-Fe_2O_3 NPs surface within the pH range of 2.00-8.00. The removal percentage gradually decreased as the pH increased. The maximum removals of the Pb^{2+}, Hg^{2+} and Cd^{2+} ions were at pH values of 4.0, 5.0 and 6.0, respectively.

2. Effect of the contact time

The experiments were performed for the adsorption of 20 mg/100 mL of Pb^{2+}, Hg^{2+} and Cd^{2+} ions at pH = 4.0–6.0 using an adsorbent dosage of 50 mg of α-Fe_2O_3 NPs. The effect of the contact time on the adsorption of these ions by α-Fe_2O_3 NPs was examined from 10 to 60 min., and represented in Figure 7. It has been found that the adsorption process increased and reached a maximum removal value of ~ 99% after 40 min.

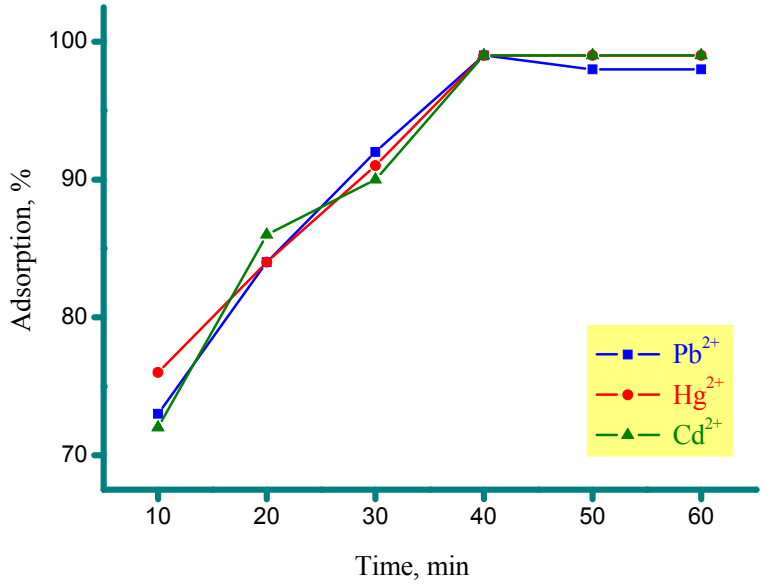

Fig. 7 – Effect of contact time on the adsorption of Pb^{2+}, Hg^{2+} and Cd^{2+} ions by α-Fe_2O_3 NPs.

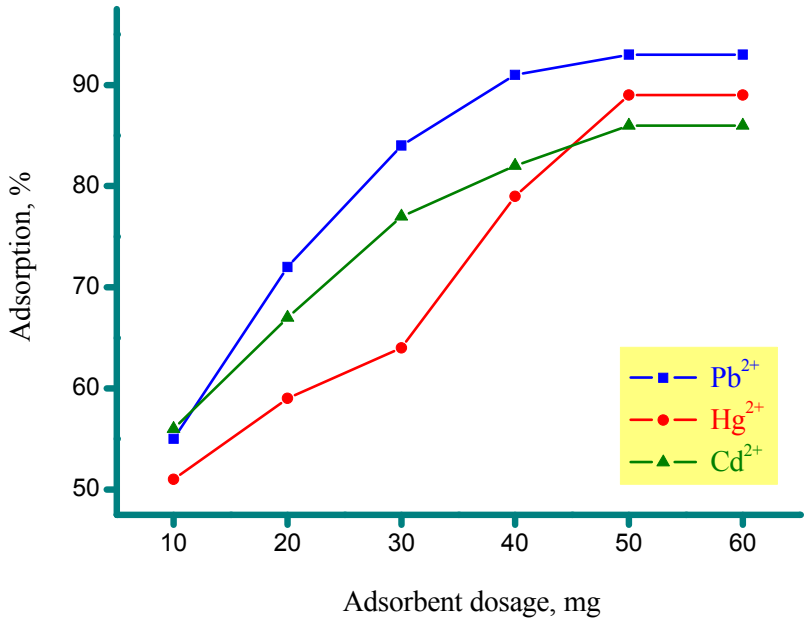

Fig. 8 – Effect of adsorbent dosage of α-Fe_2O_3 on the adsorption of Pb^{2+}, Hg^{2+} and Cd^{2+} ions.

Table 2

Electrical conductivity results of iron(III) complexes

Complexes	**δ, ohm^{-1}**	**E_1, eV**	**E_2, eV**	***n*, cm^{-3}**	**μ, cm^2/V.s.**
1	1.92E-06	0.49	0.29	1.45E20	7.98E-08
2	1.54E-06	0.17	0.14	1.02E25	2.02E-012

1- $[Fe_3(\mu\text{-}CO_3)(NH_3)(\mu\text{-}OH)_2(H_2O)_5(\mu\text{-}H_2O)(OH)_4]Cl{\cdot}6H_2O$ complex, 2- $[Fe_3(\mu\text{-}CO_3)(NH_3)(\mu\text{-}OH)_2(H_2O)_5\ (\mu\text{-}H_2O)(OH)_4]NO_3{\cdot}6H_2O$ complex.

3. Effect of the adsorbent dosage

Figure 8 shows the effect of adsorbent dosage of α-Fe_2O_3 NPs on the adsorption of Pb^{2+}, Hg^{2+} and Cd^{2+} ions. It has been found that the removal efficiency of Pb^{2+}, Hg^{2+} and Cd^{2+} ions increased in proportion to the amount of the adsorbent until a certain value was reached. After that, the removal efficiency was constant even if more adsorbent was added. The removal efficiency rapidly increased with the increase in the adsorption of the adsorbent due to the increased availability of absorption sites on the surface area. The experimental study showed that the appropriate dose of α-Fe_2O_3 NPs as a good adsorbent for each of the heavy metal ions is 50 mg.

4. Optimum conditions

The α-Fe_2O_3 NPs prepared through the thermal decomposition method showed promising results for the investigated heavy metals in aqueous media. Nearly 93, 89 and 86% removal efficiencies for Pb^{2+}, Hg^{2+} and Cd^{2+} ions, respectively, were achieved using the synthesized α-Fe_2O_3 NPs with a low weight of adsorbent (~ 50 mg), short time (40 min.) and at pH values ranging from 4.0-6.0. The optimum conditions for the efficiency removal of these heavy metals were: an adsorbent dosage of 50 mg, a contact time of 40 min., and a pH of 5.0. The thermal decomposition of the synthesized Fe-urea complexes produced pure α-Fe_2O_3 NPs in good agreement with the previously results reported [20-23, 25, 29]. The obtained α-Fe_2O_3 product was used as adsorbent for water treatment, and the results revealed excellent performance for heavy metal removal in accordance with previously works.[25,29]

8. Electrical conductivity

The general equation that used to identify the electrical behavior associated with the movement of electrons can be cited as:

$$\sigma = q\ n\ \mu$$

where (σ = conductivity, q = charge, n = concentration, and μ = mobility of charge carrier).

The electrical conductivity value was calculated dependent on the following equation:

$$\sigma = \sigma^{o} \exp(-E/KT)$$

where (σ^{o} = constant and E = activation energy).

The conductivity value increases with the increasing of temperature. So, the solid iron(III) complexes have a semi-conductance behavior. It is found that the conductivity values for $[Fe_3(\mu\text{-}CO_3)(NH_3)(\mu\text{-}OH)_2(H_2O)_5(\mu\text{-}H_2O)(OH)_4]Cl\cdot 6H_2O$ and $[Fe_3(\mu\text{-}CO_3)(NH_3)(\mu\text{-}OH)_2(H_2O)_5(\mu\text{-}H_2O)(OH)_4]NO_3\cdot 6H_2O$ complexes are different dependent on the various of anions outside the coordination sphere. The stability of complexes increased with decreasing the conductivity according to the decreasing in electronic mobility. The electronic conductivity data are listed in Table 2. The conductivity measurement of $[Fe_3(\mu\text{-}CO_3)(NH_3)(\mu\text{-}OH)_2(H_2O)_5(\mu\text{-}H_2O)(OH)_4]Cl\cdot 6H_2O$ complex is lesser than $[Fe_3(\mu\text{-}CO_3)(NH_3)(\mu\text{-}OH)_2(H_2O)_5(\mu\text{-}H_2O)(OH)_4]NO_3\cdot 6H_2O$ complex. This result can be assigned to the electronegativity and inductive impact of anions (Cl^-/NO_3^-). The data of mobility for charge carriers was calculated using the following equation:

$$n = 2(2\pi m^{+} KT / h^2)^{3/2} e^{-E/KT}$$

where (m^+ = effective mass of charge carrier). From Table 2, the mobility results $\mu(cm^2/V.s.)$ have low data within (10^{-8}-10^{-12}). These physical data reveal that, the conduction of solid iron(III) complexes occurs by hopping mechanism. The conduction through the localization electrons denote discrete jumps across an energy barrier from one site to other one. It is obvious that the hopping conduction mechanism can be used to described the electrical behavior of the iron(III) complexes.

CONCLUSION

Two new complexes of iron(III) ions were prepared using urea at ~ 50 °C. The obtained complexes were characterized using elemental and thermal analyses as well as FT-IR spectroscopy. The two complexes were decomposed at 600 °C in a static air atmosphere. The XRD and SEM analyses indicated that the decomposition product is α-Fe_2O_3 NPs with an average particle size of ~ 14 nm. The performance and capacity of the α-Fe_2O_3 NPs for the removal of Cd^{2+}, Pb^{2+} and Hg^{2+} ions from wastewater were studied. The optimum pH value, contact time, and adsorbent dose for the maximum possible removal of these metal ions were investigated. The adsorption capacity of the α-Fe_2O_3 NPs for the metal ions was in the following order: Pb(II) > Hg(II) > Cd(II).

Acknowledgements. This work was supported by grants from Vice President for Graduate Study and Research, Taif University, Saudi Arabia under project Grants No. 5558-438-1.

REFERENCES

1. B. A. Lajayer, M. Ghorbanpour, S. Nikabadi, *Ecotox. Environ. Safe.*, **2017**, *145*, 377-390.
2. I. A. Aguayo-Villarreal, A. Bonilla-Petriciolet, R. Muñiz-Valencia, *J. Mol. Liq.*, **2017,** *230*, 686-695
3. H. Xiyili, S. Çetintaş, D. Bingöl, *Process Saf. Environ. Protection*, **2017**, *109*, 288-300.
4. J. L.G. Fierro, Metal Oxides: Chemistry and Applications"", CRC Press, Florida, 2006.
5. V. E. Henrich, P. A. Cox, "The Surface Chemistry of Metal Oxides, Cambridge University Press, Cambridge, UK, 1994.
6. C. Noguera, Physics and Chemistry at Oxide Surfaces"", Cambridge University Press, Cambridge, UK, 1996.
7. A. R. José and F.-G. Marcos, "Synthesis, Properties, and Applications of Oxide Nanomaterials", Willey, New Jersey, 2007.
8. J. Hu, M. C. I. Lo and G. Chen, *Sep. Purif. Technol.*, **2007,** *56*, 249-256.
9. X. Wang, C. Zhao, P. Zhao, P. Dou, Y. Ding and P. Xu, *Bioresour. Technol.*, **2009**, *100*, 2301-2304.
10. K. L. Palanisamy, V. Devabharathi, N. M. Sundaram, *Int. J. Research in Appl., Natural and Social Sci.* (IMPACT: IJRANSS), **2013,** *1*, 15-22.
11. G. Ertl, H. Knozinger and J. Weitkamp, "Handbook of Heterogeneous Catalysis", Wiley-VHC, Weinheim, 1997.
12. J.-P. Jolivet, "Metal Oxide Chemistry and Synthesis: From Solution to Solid State", Wiley, Chichester, 2000.
13. Z. Zheng, "Synthesis and Modifications of Metal Oxide Nanostructures and Their Applications", *PhD thesis,* School of Physical and Chemical Sciences, Queensland University of Technology, 2009.
14. I. Sheet, A. Kabbani and H. Holail, *Energy Procedia*, **2014**, *50*, 130-138.
15. D. Inthorn, Y. Tani, J. Chang, H. Naitou and N. Miyata, *J. Environ. Chem. Eng.,* **2014,** *2,* 1635-1641.
16. E-B. Son, K-M. Poo, J-S. Chang and K-J. Chae, *Sci. Total. Environ.,* **2018,** *615*, 161-168.
17. S. Lin, L. Liu, Y. Yang and K. Lin, *Appl. Surf. Sci.*, **2017**, *407*, 29-35.
18. H. Su, Z. Ye and N. Hmidi, *Colloids Surf. A: Physicochem. Eng. Asp.*, **2017**, *522*, 161-172.
19. M. Ocana, M. P. Morales and C. J. Serna, *J. Colloid Interface Sci.,* **1998,** *212*, 317-323.
20. S. Bakardjieva, V. Štengl, J. Šubrt and E. Večerníková, *Solid State Sci.*, **2005**, *7*, 367-374.
21. S. Asuha, S. Zhao, H.Y. Wu, L. Song and O. Tegus, *J. Alloys Compd.*, **2009**, *472*, L23-L25.
22. S. Zhao, H.Y. Wu, L. Song, O. Tegus and S. Asuha, *J. Mater. Sci.*, **2009**, *44*, 926-930.
23. S. Asuha, S. Zhao, X. H. Jin, M. M. Hai and H. P. Bao, *Appl. Surface Sci.*, **2009,** *255*, 8897-8901.

24. N. Jović, N. Cvjetićanin, B. Babić-Stojić, D. Makovec and V. Jokanović, *Ceram. Int.*, **2013**, *39*, 5659-5665.
25. H. Liang, B. Xu and Z. Wang, *Mater. Chem. Phys.,* **2013**, *141*, 727-734.
26. N. N. Mallikarjuna, A. Venkataraman, *Talanta*, **2003**, *60*, 139-147.
27. C. M. Gonzalez, J. Hernandez, J. R. Peralta-Videa, C. E. Botez, J. G. Parsons and J. L. Gardea-Torresdey, *J. Hazard. Mater.*, **2012,** *211-212*, 138-145.
28. B. Prasad, C. Ghosh, A. Chakraborty, N. Bandyopadhyay and R. K. Ray, *Desalination*, **2011**, *274,*105-112.
29. D. Wang, P. Yang and B. Huang, *Mater. Res. Bull.*, **2016,** *73*, 56-64.
30. P. F. Selwood, "Magnetochemistry", 2nd edition, Wiley (Interscience), N.Y., 1956.
31. K. Nakamoto, "Infrared and Raman Spectra of Inorganic and Coordination Compounds", Wiely, New York, 1978.
32. S. D. Ross, "Inorganic Infrared and Raman Spectra", Mc Graw Hill, London, 1972.
33. M. K. Chaudhuri, S. K. Ghosh, *Polyhedron*, **1982**, *1*, 553-555.
34. R. B. Penland, S. Mizushima, C. Curran, J. V. Quagliano, *J. Am. Chem. Soc.*, **1957**, *79*, 1575-1578.
35. D. Forster, W. D. Harrocks Jr., *Inorg. Chem.*, **1967**, *6,* 339-343.
36. V. Vogel, "Qualitative Inorganic Analysis", John Wiely & Sans, Inc. New York, 1987.
37. W. J. Geary, *Coord. Chem. Rev.*, **1971**, *7*, 81-122.
38. A. D. Kulkarni, S. A. Patil and P. S. Badami, *Int. J. Electrochem. Sci.*, **2009**, *4*, 717-729.
39. C-Y. Cao, J. Qu, W-S. Yan, J-F. Zhu, Z-Y. Wu and W-G. Song, *Langmuir*, **2012**, *28*, 4573-4579.
40. H. P. Klug, (Ed.), "X-ray Diffraction Procedures for Polycrystalline and Amorphous Materials", New York, Wiley, 1974.
41. E. Vélez, G. E. Campillo, G. Morales, C. Hincapié, J. Osorio, O. Arnache, J. I. Uribe and F. Jaramillo, *J. Phys.: Conf. Ser.*, **2016**, *687*, 012050.
42. J. Tauc, *Mater. Res. Bull.*, **1968**, *3*, 37-46.
43. B. Gilbert, C. Frandsen, E. R. Maxey and D. M. Sherman, *Phys. Rev. B*, **2009**, *79*, 035108.
44. M. P. Dare-Edwards, J. B. Goodenough, A. Hamnett, P. R. Trevell, *J. Chem. Soc., Faraday Trans.*, **1983**, *79*, 2027-2041.